

## **Chromatic adaptation for robust visual navigation**

GIOVANNI M. BIANCO<sup>1,\*</sup> and ALESSANDRO RIZZI<sup>2</sup>

<sup>1</sup> *University of Verona, Computer Science Service, Via San Francesco 22, 37129 Verona, Italy*

<sup>2</sup> *University of Milano, Department of Information Technology, Via Bramante 65, 26013 Crema, Italy*

Received 29 January 2001; accepted 21 July 2001

**Abstract**—This paper analyzes the effects of the application of visual adaptation mechanisms on snapshot-based guidance methods. The guidance principle of the visual homing is proven to be a visual potential function with an equilibrium point located at the goal position. The presence of a potential function means that classical control theory principles based on the Lyapunov functions can be applied to assess the robustness of the navigation strategy. The Retinex algorithm, a blind chromatic equalization pre-filtering that performs color constancy with no *a priori* information about the illuminant, is proposed as an unsupervised visual adaptation mechanism. It increases the visual information similarity under changes in the illuminant, thus increasing the robustness of the visual guidance. Tests and comparisons are presented.

*Keywords:* Visual navigation; color equalization; Retinex; Lyapunov function; potential field.

### **1. INTRODUCTION**

Thanks to entomological studies on animals, several mechanisms of visual guidance can be effectively applied to robotics, e.g. [1] and review in [2]. Furthermore, studies involving human vision system adaptation mechanisms can offer valuable ideas for visual filtering algorithms that can be suitably and effectively used to improve vision based motion strategies [3].

Among the former, practical implementations of some methods can be effectively used on real robots [4, 5]. Basically, the implemented methods are 2-fold: first match, then navigate. The latter is driven by the differences discovered in the matching phase. The differences need to be measurable so that proper movements can reduce the discrepancies between the images.

In [6] a formal theory that explains the experiments conducted in [4, 5] has been introduced. Basically, it analyzes the underlying principle that drives the robot to the

---

\*To whom correspondence should be addressed. E-mail: giovanni.bianco@univr.it

goal, basing all the assumptions on the presence of a navigation vector field whose basin of attraction is placed at the goal position. A potential function is numerically computed starting from the navigation vector field and its presence around the goal position is a sufficient condition for classical control theory methods such as the Lyapunov functions. Therefore, important considerations on the robustness of the homing methods can be introduced.

Regarding the visual adaptation mechanisms, they can play an important role in any vision-driven task, visual guidance included. A good example of implementation of biologically based adaptation mechanisms can be found in the Retinex algorithm. Basically, the Retinex algorithm acts similarly to adaptation mechanisms present in the human vision system. These cause the user to perceive the relative chromaticity of an area, rather than its absolute color. Furthermore, the Retinex algorithm is also invariant with respect to chromatic dominants and it does not require any *a priori* knowledge of the acquisition process.

As an extension of the studies performed in [6], the aim of the present paper is to analyze the effects of the Retinex pre-filter for snapshot-based guidance planners. We will show how the effects of the Retinex pre-filtering can be well measured according to the theory introduced in [6].

The organization of this paper is as follows. A brief introduction to related works is presented in Section 2, then an overview of the visual potential function theory is addressed in Section 3. A review of the snapshot-based homing strategy adopted is detailed in Section 4. The problems related to the use of color in visual navigation along with the Retinex algorithm chosen for the color normalization are described in Section 5. Comments on a set of the experiments and tests conducted, and remarks about future work conclude the paper.

## 2. RELATED WORKS

In order to make a planning problem tractable, most techniques make use of strong simplifying hypotheses [7], that describe the environment with well-known and deterministic dynamics. To operate in a real world, however, planning with uncertainties must assume more and more importance.

The approaches followed to limit uncertainties and ambiguities arising from vision mainly treats data on the fly through the use of diverse techniques. For example, the use of Bayesian learning [8–10] to solve localization problems, or the use of geometrical representation for constellations of landmarks to solve problems related to their match [11, 12], or the use of Fuzzy controllers [13] that can be coupled with Neural Networks [14]. Among them, recently, qualitative techniques seem to have gained more interest than quantitative techniques based on high-precision control methods.

Landmarks for visual navigation can be selected in a great variety of ways, either using natural or pre-engineered features (e.g. [9, 15, 16]). Following a qualitative

approach, we propose a biological inspired robot navigation [5], but our goal is to improve and to verify the robustness of the method.

The approach presented in this paper introduces two novel ways of improving and keeping under control the robustness of an agent. The first is an unsupervised chromatic correction algorithm that enhances the visual information at the sensor level, increasing in this way the image information content. The second is a formal framework developed to detect the robustness improvement introduced in a visual navigation algorithm.

This framework uses the Lyapunov function to study in a unified manner the behavior of a given (non-linear) system providing the area of convergence, the degree of convergence and the stability of the system itself [17, 18].

In order to cope with uncertainties on sensors, devices and dynamics, several approaches have been proposed (review in [19, 20]). Our approach tries to enhance the visual information at the sensor level by pre-filtering the grabbed images in order to equalize their chromatic content. The chromatic filtering has been introduced to compensate the unwanted color shifts deriving from natural or human-driven changes in the illuminant spectral composition. Usually, when a light spectral composition change is known, it is corrected with a linear approximation [21] of the color RGB triplets that can be acceptable for most of the visual navigation algorithms. In this case, even if the corrected images are suitable for the visual navigation algorithm, the overall robustness of the method can decrease.

When the spectral composition of the light is unknown, a color constancy algorithm can be used. The unsupervised color constancy approaches with no *a priori* knowledge about the illuminant can be divided into two categories. The algorithms that estimate the illuminant using the constraints on the physics of the scene [22], or on the spectral matching between the image and all the possible illuminants [23], or using statistic techniques [24], follow the first approach. This quantitative approach primarily considers the color constancy phenomenon from a physical aspect. On the contrary, the second qualitative approach is based on the ratio of the image areas and follows the adaptation mechanisms of the human visual system. Among the various theories that follow the second approach, there is Retinex, developed by Edwin Land [25]. In fact, the Retinex theory assumes that color perception is based on ratios of reflected light intensity in specific wavelength bands computed between adjacent areas and not of its spectral power distribution, and that is in line with the biological inspiration of the chosen method.

### 3. PRINCIPLES

An agent computes a vector using local sensor information then the next movement is performed. If vector  $\vec{V}$  represents the next movement, with a module and a direction relative to the actual robot position, considering an agent with 2 d.o.f., for the sake of simplicity, the system dynamical model to perform guidance is therefore

given by:

$$\begin{cases} x(k+1) = x(k) + V_x(x(k), y(k)) \\ y(k+1) = y(k) + V_y(x(k), y(k)), \end{cases} \quad (1)$$

where  $x(k)$  and  $y(k)$  represent the coordinates of robot at step  $k$ ;  $x(k+1)$  and  $y(k+1)$  represent the new positions the robot will move to. Clearly, an important equilibrium point  $(x^*, y^*)$  for the system is given by the coordinates of the goal position.

Lastly,  $V_x(x(k), y(k))$  and  $V_y(x(k), y(k))$  represent the displacements computed at step  $k$  following a generic guidance model. Those displacements are related to the position at step  $k$  given by  $(x(k), y(k))$ .

The computation over the whole environment of vector  $\vec{V}$  defines a vector field  $\mathbf{V}$ . Several interesting considerations can be suitably extracted by analyzing its properties.

Let us consider a partial set of equivalent statements about a generic vector field  $\mathbf{V}$  [27].

- Any oriented simple closed curve  $c$ :  $\oint_c \mathbf{V} \cdot d\mathbf{s} = 0$ ,
- $\mathbf{V}$  is the gradient of some function  $U$ :  $\mathbf{V} = \nabla U$ .

Both these conditions are of utmost importance for guidance strategies.

The former is related to the concept of *conservativeness* of the field. The latter is concerned with the existence of a *potential function* that uniquely generates the field. From another point of view, the former is concerned with the repeatability of the experiments, the latter is concerned with their convergence to the goal.

The following sections address the two aspects.

### 3.1. Convergence

Supposing that all the necessary hypotheses hold, the dynamic system presented in (1) can be considered continuous-time with the following (omitting the vector notation):

$$\dot{x}(t) = V(x(t)), \quad (2)$$

where  $x$  represents the generic coordinates and an equilibrium point  $x^*$  is located at the goal position. The basic idea for verifying the stability and the convergence of a dynamic system is to seek an aggregate summarizing function on the states of the system itself [26]. This happens, in particular, when a dynamic system can be represented by  $\dot{x} = f(x)$  with a fixed point  $x^*$ , and it is possible to find a *Lyapunov function*, i.e. a continuously differentiable, real-valued function  $U(x)$  with well-known properties [26]:

- (i)  $U(x) > 0$  for all  $x \neq x^*$  and  $U(x^*) = 0$ ,
- (ii)  $\dot{U}(x) < 0$  for all  $x \neq x^*$  and  $\dot{U}(x^*) = 0$  (all trajectories flow *downhill*)

then  $x^*$  is globally stable: for all initial conditions  $x(t) \rightarrow x^*$  as  $t \rightarrow \infty$ . The system depicted in (2) is of type  $\dot{x} = f(x)$  but, unfortunately, there are no systematic ways to construct Lyapunov functions.

In our case, by considering the vector field the guidance system produces, an important Lyapunov function can be constructed by integrating the right-hand side of the system (2) as reported in [26].

Our approach consists of calculating the shape of  $U$  *a posteriori*, starting from the vector field  $\mathbf{V}$ . Classically,  $U$  is mathematically specified once given the sensors and the environment [19]. The scalar function  $U$  can thus be given by integrating the conservative field  $\mathbf{V}$  in question, taking into account that the field must be inverted in sign [19]:

$$U(x, y) = - \int_{(0,0)}^{(x,y)} \mathbf{V} \, ds, \quad (3)$$

where the path of integration, following the infinitesimal piece of motion  $ds$ , is arbitrary. Scalar function  $U$  is referred to as the *potential* of the conservative field  $\mathbf{V}$  in question.

The scalar product reported by (3) can be further simplified by following a *particular* curve  $c$ . Therefore, more effectively, it can be written as:

$$U(x, y) = - \int_{p_x}^x V_x(X, p_y) \, dX - \int_{p_y}^y V_y(x, Y) \, dY, \quad (4)$$

where  $U(x, y)$  is the potential function and the path of integration is along the semi-perimeter of the rectangle connecting  $(p_x, p_y)$  to  $(x, y)$ , i.e. the horizontal line segment from the initial point  $(p_x, p_y)$  to the vertical line through  $(x, y)$  and then along the vertical line segment to  $(x, y)$ .

An advantage of this method is the use of the goal position as the reference point  $(p_x, p_y)$ . Every other point is thus referred to in terms of potential in reference to the goal position. If the visual potential function has a basin of attraction where the minimum is at the goal position then for the considerations expressed above homing is intrinsically stable, when starting navigation from part of the environment.

### 3.2. Repeatability

As described above, a vector field  $\mathbf{V}$  is said to be *conservative* when the integral computed on any closed path (*circulation*) is zero.

If the field is not conservative (when the equation stating that the circulation is null does not hold for at least one curve) then the integration detailed in (3) can lead to an infinite number of results depending on the integrating curve  $c$ . This means that the potential function is no longer entirely determined by the extreme points of the integration process. This potential function can be considered as *multi-valued*: for every reference position, a general position will have more than one potential value according to the path chosen for integration. This sort of

multi-valued potential function can be translated in *non-uniqueness* of the vector field. In other words, repeatedly placing the robot in the same point within a non-conservative area, different paths can be followed. Theoretically, as the field is not unique, the repeatability of navigation paths does not hold and this can lead to unpredictable results.

A practical measure of the conservativeness of the field appears to be essential to assess the quality of the navigation process. To this extent, if the vector field is defined on a connected set then the equation stating that the circuitation must be null is equivalent to [27]:

$$\frac{\partial V_x(x, y)}{\partial y} = \frac{\partial V_y(x, y)}{\partial x}. \quad (5)$$

In other terms:

$$\frac{\partial V_x(x, y)}{\partial y} - \frac{\partial V_y(x, y)}{\partial x} = 0. \quad (6)$$

Hereafter, the result of (5) will be referred to with the term of *conservativeness*.

#### 4. SNAPSHOT-BASED GUIDANCE

In this Section we present the model of visual guidance. Details of the theory and the experiments can be found in [4, 5].

The main idea is that an estimate of the vector pointing from the current position of the agent to the pre-learned goal can be computed comparing position and amplitude of matching areas in the considered images. The matching between the goal image and the actual view is performed using an affine model. From the parameters of the affine transformation the algorithm computes an estimate of the robot displacement from the goal position, i.e. its current position. Part of the goal panorama (depending on the contest) must be present in the actual view for the matching to produce valuable estimates.

Some constraints, i.e. fixed heading and constant height of the camera, allow for the use of a simplified affine model for matching:

$$\begin{cases} S_X(X, Y) = a_{0X} + a_{1X} \cdot X + a_{2X} \cdot Y \\ S_Y(X, Y) = a_{0Y} + a_{1Y} \cdot X + a_{2Y} \cdot Y, \end{cases} \quad (7)$$

where  $S_X$  and  $S_Y$  are the displacement components for the matching along  $x$  and  $y$  axes respectively;  $(X, Y)$  are the pixels coordinates,  $a_{0X}$ ,  $a_{0Y}$  represent translations in pixels and  $a_{1X}$ ,  $a_{2X}$ ,  $a_{1Y}$ ,  $a_{2Y}$  represent expansions (a-dimensional).

Furthermore, other working hypotheses allow for additional simplifications of the affine model [5]. The computation of the estimated displacement components from the actual position of the agent to the goal is given by:

$$\vec{V} = [V_x \ V_y] = [K \cdot a_{0X} \ H \cdot a_{1X}], \quad (8)$$

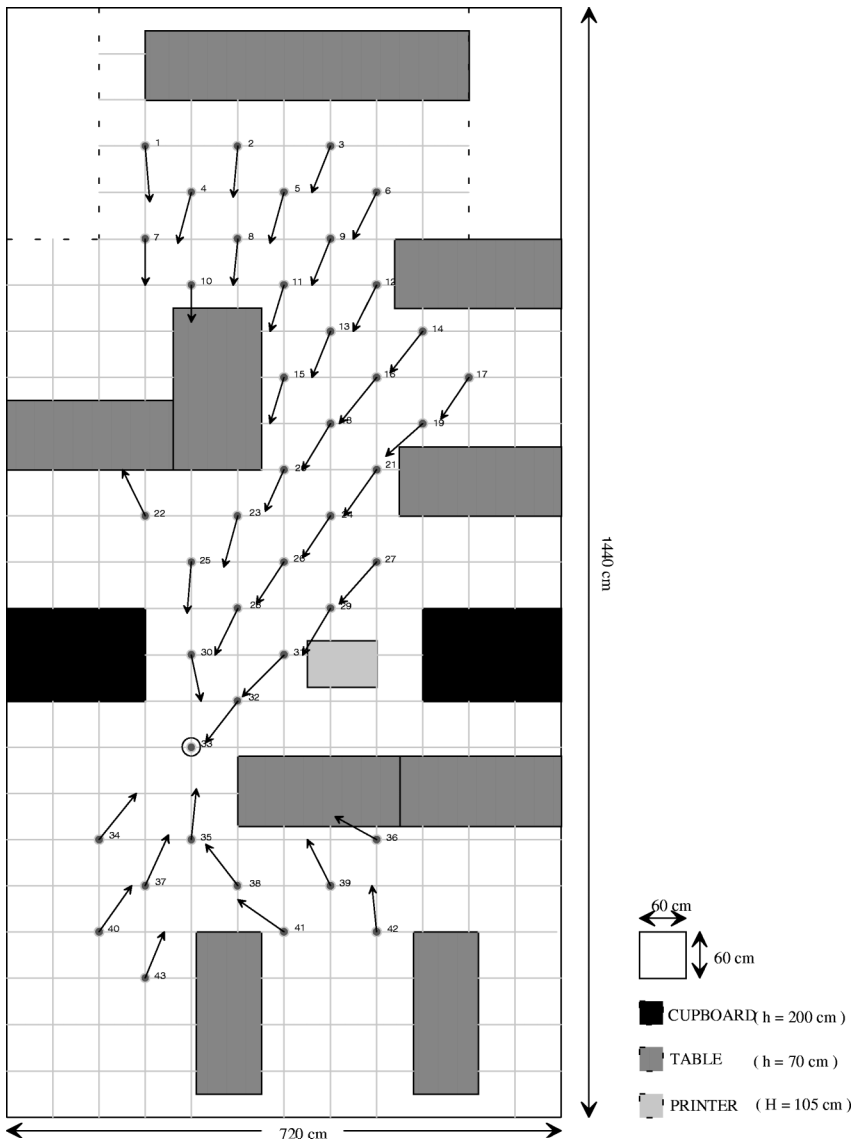


**Figure 1.** An example of a navigation field.

where  $K$  and  $H$  are constants which derive from the central projection theorem as reported in [5].

In Fig. 1, the directions of the estimated displacement vectors  $\vec{V} = [V_x V_y]$  for the first navigation steps from a group of starting points are shown. The goal (represented by a small circle) seems to be located within a basin of attraction.

## 5. THE RETINEX MODEL

Consider a spectral distribution of the illuminant light is  $E(\lambda)$  and  $R^x(\lambda)$  is the reflectance of the surface at a point  $x$ . Therefore, the reflected light spectral distribution grabbed by the camera is:

$$C^x(\lambda) = E(\lambda)R^x(\lambda).$$

The color constancy problem arises when the ambient light spectral power distribution  $E(\lambda)$  is not known and  $R^x(\lambda)$ , which determines the color, has to be estimated from the perceived color signal. It usually happens when the light spectral composition changes, i.e. due to light bulbs turned on, sun dawning through the windows or emergency lights working.

To compute the corresponding color, several solutions have been proposed, but most of them need information about the illuminant spectral shift. The Retinex algorithm does not need any *a priori* information in order to discount the illuminant of the scene. In fact it tries to simulate how the human vision system can estimate the chromatic dominant, assuming the color perception as the result of complex comparisons among different visual areas [28].

Figures 2 and 3 show an example of application of the Retinex algorithm. The Fig. 2 shows some images grabbed at the same navigation point under different light conditions and with different white balance corrections, using automatic exposure and without any gamma correction. Figure 3 shows the same image filtered by



**Figure 2.** Image viewed by the camera: normal light.



**Figure 3.** Image viewed by the camera pre-filtered with Retinex.

Retinex. As can be noticed, the color difference between the images greatly decreases.

Different software [29, 30] and hardware [31] implementations of the Retinex theory have been developed so far; our approach differs from the previous ones in the way the image is ‘explored’ by the algorithm. More attention has been paid in keeping the computation as close as possible to some recent biological models of color perception [32, 33].

### 5.1. The Retinex algorithm

According to the Retinex theory, every color sensation derives from the processing of three independent stimuli in the three different retinal cones wavebands (approximately red, green and blue) [34]. For each channel, the relative lightness of a pixel is computed as the mean value of the relative lightness along a number  $N$  of random paths across the image, ending at that pixel (Fig. 4, left side).

Hence, using Retinex as a model of the cortical computation, the ‘perceived’ RGB intensity values ( $\hat{I}$ ) for each point  $i$  is the mean value of relative lightnesses  $l_{R,G,B}^{i,j}$  computed over a number  $N$  of random paths (Fig. 4, left side) ending at point  $i$ , separately for each RGB channel:

$$\hat{l}_{R,G,B}^i = \frac{\sum_{k=1}^N l_{R,G,B}^{i,j_k}}{N},$$

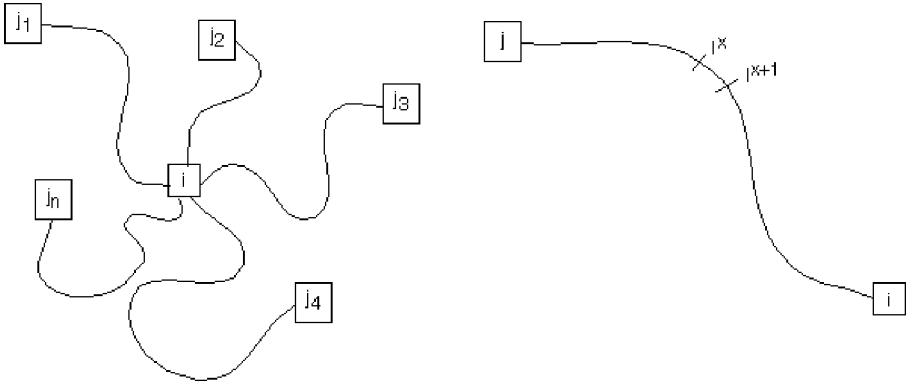


**Figure 4.** Left: random paths to pixel  $i$ . Right: chain computation for path  $i - j$ .

with:

$$I_{R,G,B}^{i,j} = \sum_{x \in \text{path}} \delta \log \frac{I^{x+1}}{I^x},$$

where, for each chromatic channel RGB,  $I^x$  is the original pixel channel value at the location  $x$ ,  $I^{x+1}$  the value at the following location  $x + 1$  along the random path (Fig. 4, right side) and  $\delta$  is a threshold value computed in the following way:

$$\delta = \begin{cases} 1 & \text{if } \left| \log \frac{I^{x+1}}{I^x} \right| > \text{threshold} \\ 0 & \text{if } \left| \log \frac{I^{x+1}}{I^x} \right| < \text{threshold}. \end{cases}$$

These computations are executed independently for the three fundamental channels RGB.

As seen in the formula above, Retinex has a reset mechanism: if during a path computation a lighter area is found, the cumulated relative lightness is forced to zero, making the average computation restart from this area. The effect of the reset mechanism is to consider the lightest area of an image as the reference value of the color white.

A critical problem in the algorithm is the choice of the random path. The solution proposed in this paper is based on Brownian paths generated with the mid-point displacement technique, that mimics the distribution of the receptive field in the interested human cortical area (V4) [33].

The application of an approximated Brownian path generation to the Retinex algorithm has greatly improved the effectiveness of the algorithm and its speed [35].

The computational space complexity of the algorithm is not heavy, it requires only the memory to keep the original image and the filtered one. On the contrary, the computational time complexity is heavy: with  $k$  paths crossing  $x$  of the  $n$  pixels of the image for each pixel computation, the number of floating point pixel ratios is

$k \times x \times n$ . The value of  $x$  can be controlled by tuning the Brownian paths generation parameters (max distance, max displacement, number of displacement, ...) and  $k$  can be set as a parameter, affecting the quality of the result. A multi-scale version of the algorithm has been developed to allow effective robotics navigations [36].

## 6. TESTS

In this section we present some experiments conducted operating with the snapshot model to perform guidance. Details on the experiments can be found in [4–6]. In order to measure the vector field, the agent was manually placed at various points in the environment. The position of the agent progressively covered a grid in the environment where each cell is approximately as big as the base of the agent itself. From those points, applying one of the navigation methods, a displacement vector is computed. The iteration of the method over the whole environment and the collection of every displacement vector produces a vector field.

All the tests have been performed in the same environment where the goal position is located in coordinate (20, 30).

The Retinex pre-filtering can be applied on every light condition, since it corrects the image colors only if a chromatic dominant is present. We applied the algorithm on the usual light conditions of our robotic laboratory and other indoor environments (daylight through the windows, tungsten and fluorescent bulbs in different mix), as in other previous experiments [3].

The first couple of figures, e.g. Figs. 5 and 6, show the conservativeness and the potential function respectively. This example does not consider any pre-filtering application of Retinex.

Figures 7 and 8, instead, show the same functions operating with the Retinex pre-filtering.

An immediate comparison can be made. From the Lyapunov function point of view, the potential function calculated with the pre-filtering has a better shape than the one computed without Retinex. This automatically leads to an improvement of the convergence to the target. Another aspect is related to the conservativeness, although a small portion of the figure shows unsatisfactory results. Nevertheless, for most of the environment the amount of conservativeness using the pre-filtering is closer to zero than when no pre-filtering is used.

## 7. CONCLUSION AND PERSPECTIVES

This paper shows how biologically inspired methods both for navigating and for enhancing visual systems can be extremely valuable for real robot applications. The behavior of these methods can be explained in terms of a visual potential function.

The presence of a potential function around the goal allows us to apply classical control theories to assess the robustness of the system such as the Lyapunov functions.

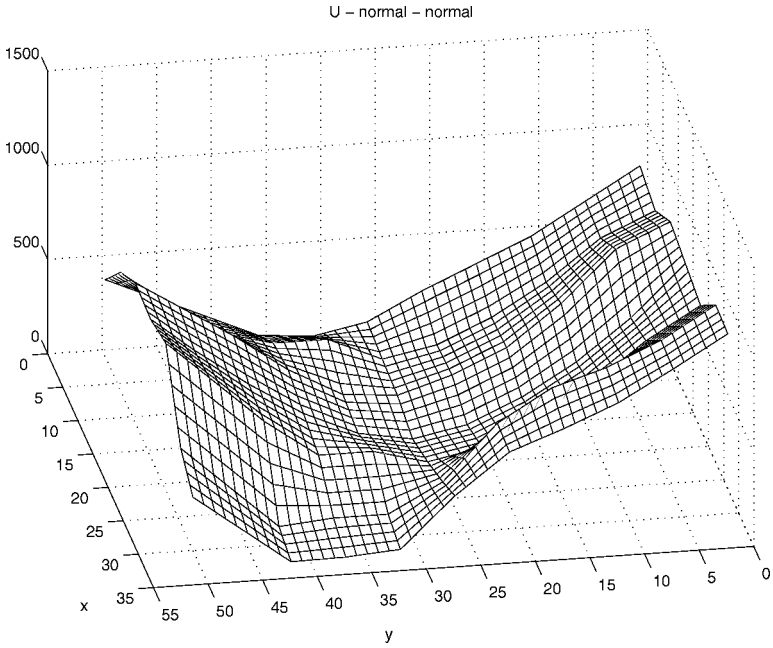


Figure 5. The visual potential function when no pre-filtering is applied. Light is normal.

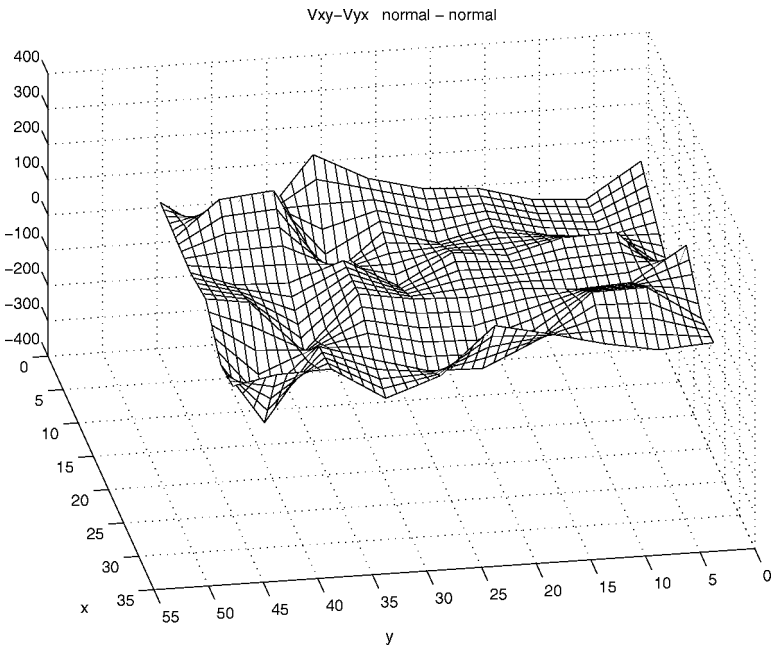
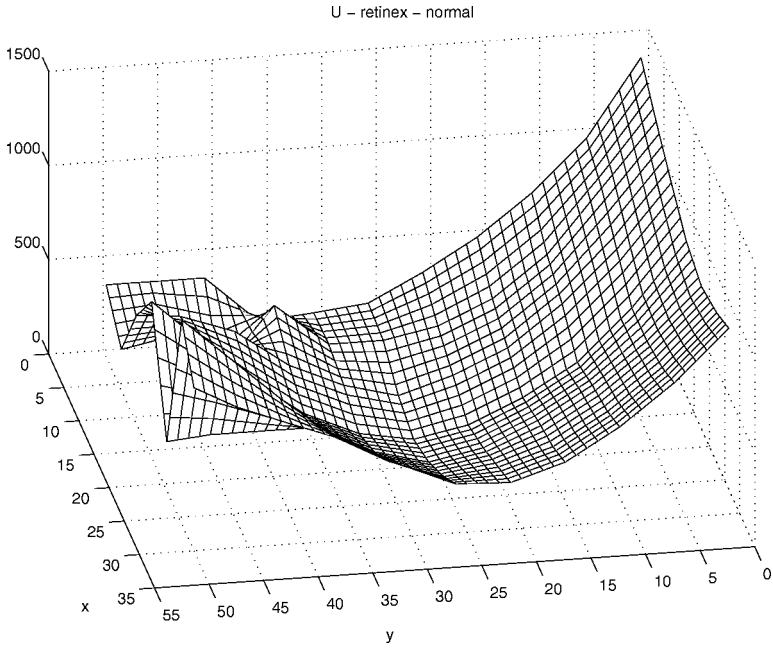
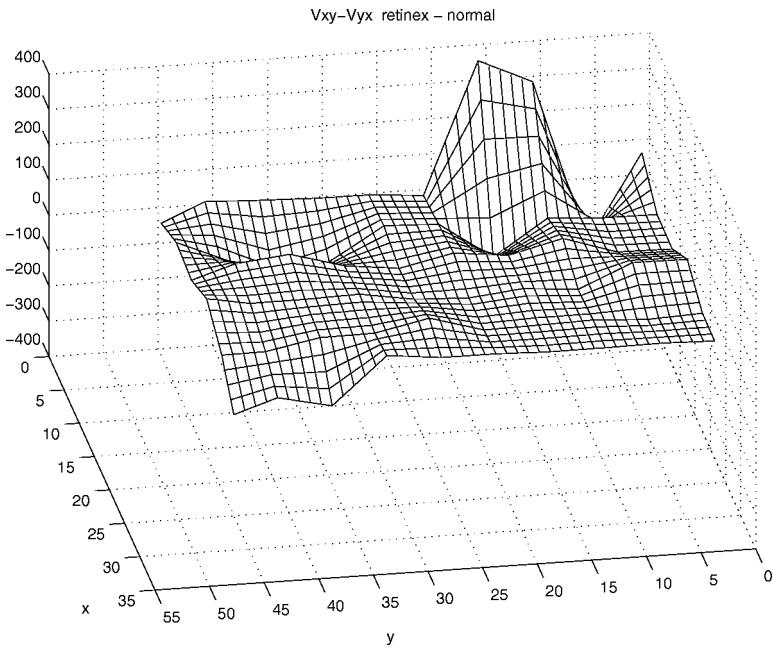


Figure 6. The conservativeness when no pre-filtering is applied. Light is normal.



**Figure 7.** The visual potential function when pre-filtering is applied. Light is normal.



**Figure 8.** The conservativeness when pre-filtering is applied. Light is normal.

A blind chromatic correction of the images grabbed by the robot during the navigation improves the effectiveness of the visual potential field navigation function. In fact, a chromatically stable environment allows a more precise matching of the visual features used to estimate the robot position.

This is consistent with the biological inspiration of the navigation approach [37].

## REFERENCES

1. M. Srinivasan, S. Zhang, M. Lehrer and T. Collett, Honeybee navigation en route to the goal: visual flight control and odometry. *J. Exp. Biol.* **199**, 155–162 (1996).
2. O. Trullier, S. Wiener, A. Berthoz and J. Meyer, Biologically based artificial navigation systems: review and prospects, *Progr. Neurobiol.* **51**, 483–544 (1997).
3. D. Marini and A. Rizzi, A computational approach to color illusion, in: *Proc. 9th Int. Conf. on Image Analysis and Processing*, Firenze, pp. 62–69 (1997).
4. G. Bianco, R. Cassinis, A. Rizzi, N. Adami and P. Mosna, A bee-inspired robot visual homing method, in: *Proc. 2nd Euromicro Workshop on Advanced Mobile Robots (EUROBOT '97)*, Brescia, pp. 141–146 (1997).
5. A. Rizzi, G. Bianco and R. Cassinis, A bee-inspired robot navigation using color images, *Robotics Autonomous Syst.* **25**, 159–164 (1998).
6. G. Bianco, A. Rizzi, R. Cassinis and N. Adami, Guidance principle and robustness issues for a biologically-inspired visual homing, in: *Proc. 3rd Workshop on Advanced Mobile Robots (EUROBOT '99)*, Zurich, pp. 143–150 (1999).
7. J. Canny, *The Complexity of Robot Motion Planning*. MIT Press, Cambridge, MA (1988).
8. F. Dellaert, W. Burgard, D. Fox and S. Thrun, Using the condensation algorithm for robust, vision-based mobile robot localization, in: *Proc. IEEE Computer Society Conf. on Computer Vision and Pattern Recognition (CVPR '99)*, pp. 588–594 (1999).
9. S. Thrun and N. Roy, Integrating learning for robust development, in: *Proc. AAAI Spring Symp.: Integrating Robotic Research*, pp. 220–225 (1998).
10. C. Olson, L. Matthies, M. Schoppers and M. Maimone, Robust stereo ego-motion for long distance navigation, in: *Proc. IEEE Computer Society Conf. on Computer Vision and Pattern Recognition*, Hilton Head, SC, pp. 453–458 (2000).
11. C. Balkenius, Spatial learning with perceptually grounded representations, *Robotics Autonomous Syst.* **25**, 165–175 (1998).
12. D. Jung, J. Heinzmann and A. Zelinsky, Range and pose estimation for visual servoing of a mobile robot, in: *Proc. IEEE Int. Conf. on Robotics and Automation*, Brussels, pp. 122–128 (1998).
13. A. Saffiotti, E. Ruspini and K. Konolige, Integrating reactivity and goal-directedness in a fuzzy controller, in: *Proc. of the 2nd Fuzzy-IEEE Conference*, San Francisco, CA, pp. 134–139 (1993).
14. J. Pan, D. Pack, A. Kosaka and A. Kak, Fuzzy-nav: a vision based robot navigation architecture using fuzzy inference for uncertainty-reasoning, in: *Proc. World Congr. on Neural Networks*, Washington, DC, Vol. 2, pp. 602–607 (1997).
15. J. Borenstein, H. Everett and L. Feng, *Where am I? Sensors and Methods for Mobile Robot Positioning*. University of Michigan Press, Ann Arbor, MI (1996).
16. G. Bianco, A. Zelinsky and M. Lehrer, Visual landmark learning, in: *Proc. IEEE/RSJ Int. Conf. on Intelligent Robots and Systems*, Takamatsu, pp. 227–232 (2000).
17. V. Balakrishnan, Robust performance bounds based on Lyapunov functions for uncertain systems, in: *Proc. Ann. Allerton Conf. on Communication, Control and Computing*, Monticello, IL, pp. 142–151 (1996).

18. G. Bianco, Biologically-inspired visual landmark learning and navigation for mobile robots, PhD thesis, Department of Engineering for Automation, University of Brescia (1998).
19. J. Latombe, *Robot Motion Planning*. Kluwer, Dodrecht (1991).
20. Y. Hwang and N. Ahuja, Gross motion planning — a survey, *ACM Comput. Surv.* **24**, 219–291 (1992).
21. J. von Kries, *Sources of Color Science*. MIT Press, Cambridge, MA (1970).
22. B. Funt, M. Drew and J. Ho, Color consistency from mutual reflection, *Int. J. Comp. Vision* **6**, 5–24 (1991).
23. G. Finlayson, P. Hubel and S. Hordley, Color by correlation, in: *Proc. 5th Color Imaging Conf.*, Scottsdale, Arizona, USA, pp. 6–11 (1997).
24. S. Tominaga and B. Wandell, Standard surface-reflectance model and illuminant estimation, *J. Opt. Soc. Am. A* **6**, 576–584 (1989).
25. E. Land, The retinex theory of color vision. *Sci. Am.* **237** (3), 2–17 (1977).
26. D. Luenberger, *Introduction to Dynamic Systems — Theory, Models, and Applications*. Wiley, New York (1979).
27. J. Marsden and A. Tromba, *Vector Calculus*. Freeman, San Francisco, CA (1996).
28. E. Land and J. McCann, Lightness and retinex theory, *J. Opt. Soc. Am.* **61**, 1–11 (1971).
29. J. J. McCann, Lesson learned from mondrians applied to real images and color gamuts, *IS&T Reporter* **14**, 1–13 (1999).
30. D. Jobson, Z. Rahman and G. Woodel, Properties and performance of a center/surround retinex, *IEEE Trans. Image Process.* (March) (1997).
31. A. Moore, J. Allman and R. Goodman, A real-time neural system for color constancy, *IEEE Trans. Neural Networks* **2**, 237–246 (1991).
32. D. Hubel, *Eye, Brain and Vision*. Freeman, New York (1988).
33. S. Zeki, *A Vision of the Brain*. Blackwell Scientific, Oxford (1993).
34. J. J. McCann, Color mondrians experiments without adaptation, in: *AIC Proc.*, Kyoto, pp. 315–322 (1997).
35. D. Marini, A. Rizzi and C. Carati, Color constancy effects measurement of the retinex theory, in: *Proc. Electronic Imaging '99, IS&T/SPIE's 11th Int. Symp.*, San Jose, CA, pp. 246–249 (1999).
36. D. Marini, A. Rizzi and L. D. Carli, Multiresolution retinex: comparison of algorithms, in: *Proc. 1st Int. Conf. on Color in Graphics and Image Processing*, Saint-Etienne, pp. 106–110 (2000).
37. W. Backhaus, A. Werner and R. Menzel, Color vision in honeybees: Metric, dimensions, constancy and ecological aspects, in: *Neurobiology and Behavior of Honeybees*, L. R. Menzel and A. Mercer (eds), pp. 172–190. Springer-Verlag (1987).

## ABOUT THE AUTHORS



**Giovanni M. Bianco** took the degree in Computer Science at University of Udine (Italy) and received a PhD in Information Engineering at University of Brescia (Italy) in 1999. He has been Professor of Algorithms and Data Structures. He was a visiting PhD student at the Australian National University in 1998 conducting research on real-time visual landmark tracking taking inspiration on Biology. Now he is leading the Computer Science Service at the University of Verona. His main research topic is biologically inspired visual robotics navigation.



**Alessandro Rizzi** took the degree in Computer Science at University of Milano and received a PhD in Information Engineering at University of Brescia (Italy) in 1999. He has been Professor of Information Systems and Computer Graphics. Now he is Assistant Professor at the University of Milano teaching Human–Computer Interaction. His main research topic is the use of color information in computer vision with particular attention to color adaptation mechanisms.